Evolution from antiferromagnetic to paramagnetic Kondo insulator with increasing hybridization; XPS studies

Evolution from antiferromagnetic to paramagnetic Kondo insulator with increasing hybridization; XPS studies

A. Ślebarski and J. Goraus
Institute of Physics, University of Silesia, Uniwersytecka 4, 40-007 Katowice, Poland

E-mail: andrzej.slebarski@us.edu.pl, jerzy.goraus@us.edu.pl

Abstract. We present the Ce 3*d* x-ray photoemission (XPS) spectra for CeM_2Al_{10} (M=Ru, Os, Fe) from which we determined the on-site hybridization between the f and conduction electron states, Δ_{cf}, and the 4f-level occupancy, n_f. Those parameters have been obtained using the Gunnarsson-Schönhammer approach. We found Δ_{cf} stronger for the Kondo insulator $CeFe_2Al_{10}$ than for the remaining compounds with Ru and Os. We discuss the type of behaviour of CeM_2Al_{10} on the base of the earlier theoretical phase diagram obtained within the Anderson-lattice model.

1. Introduction

Kondo insulators (KI) are characterized as a class of *nonmagnetic* narrow-gap Δ semiconductors and semimetals, which exhibits a metallic heavy-fermion (HF) state at temperatures $T > \Delta$[1]. Within the framework of the periodic Anderson model [2], the small energy gap in Kondo insulators arises from the strong hybridization V between the conduction band and the f-electron states. The insulating gap Δ diminishes, however, with increasing temperature [3], which indicates that its origin is not the same as in the conventional band semiconductors, instead it is a result of strong many-body correlations [4]. Most of the known Kondo insulators; e.g., CeRhSb [5] or $Ce_3Bi_4Pt_3$ [6] are paramagnetic because the magnetic moments of Ce are quenched due to the Kondo singlet state via strong hybridization between itinerant (s,p) and localized (f) states. However, Kondo semiconductors $CeRu_2Al_{10}$ [7] and $CeOs_2Al_{10}$ [8] that show anomalous magnetic phase transition at $T^* \sim 28$ K below the Kondo temperature $T_K \sim 100$ K have been found, in contrast to isostructural paramagnetic Kondo insulator $CeFe_2Al_{10}$ [9] and remaining well known KIs. The T^* phase transition was first attributed to an antiferromagnetic order of the Ce sublattice with strongly reduced magnetic moment of Ce atoms [10], while the magnetic ordering was not confirmed by NMR [11]. Very recently Kimura *et al*. suggested that the antiferromagnetic ordering at T^* in $CeOs_2Al_{10}$ [12] and $CeRu_2Al_{10}$ [13] can result from the hybridization effect between the conduction and f-electrons which causes charge-density wave (CDW) instability which can induce magnetic ordering. The nature of the T^*-phase transition has been, however, still controversial since the Ce-Ce distance in the unit cell is larger than 5 Å and Gd-based counterparts have a lower Néel temperature T_N. We try to interpret this new *magnetic* KI state on the base of the ground-state phase diagram for periodic Anderson model [2] on the V-n_e plane (n_e is the total number of electrons per site). This approach allowed to determine in the mean-field approximation the phase boundary between the antiferromagnetic Kondo-insulating state (AKI) with almost compensated magnetic moments and the paramagnetic Kondo insulator phase (for details, see [2]).Hybridization energy $\Delta_{cf} \sim$ V and the occupation number of the f shell, n_f, have been determined experimentally from the XPS

spectra using the Gunnarsson-Schönhammer (GS) approach [14]. We measured the energy Δ_{cf} for $CeRu_2Al_{10}$ and $CeOs_2Al_{10}$ significantly smaller than Δ_{sf} of $CeFe_2Al_{10}$, which inside the Anderson-lattice model [2] suggests the antiferromagnetic Kondo insulator ground state (or antiferromagnetic phase AFM2, for details see Ref. [2]) for the both *magnetic* materials and paramagnetic KI low-T state for $CeFe_2Al_{10}$. Our experimental results agree with very recent local-density approximation (LDA) band structure calculations [13], which confirmed that the hybridization energy V of $CeRu_2Al_{10}$ and $CeOs_2Al_{10}$ is slightly weaker than that of $CeFe_2Al_{10}$.

2. XPS spectra; results, analysis and discussion

Polycrystalline samples CeM_2Al_{10}; M = Ru, Os and Fe, were prepared by arc-melting stoichiometric amounts of the elemental metals in an ultra-high-purity argon atmosphere and annealing for 2 weeks at 800°C. The XPS spectra were obtained with monochromatized Al Kα radiation using a PHI 5700 ESCA spectrometer. We also measured the electrical resistivity ρ and magnetic ac susceptibility χ_{ac} using a Quantum Design PPMS platform, the results are very consistent with those, recently obtained for the polycrystalline samples.

Figure 1 compares the valence band (VB) XPS spectra obtained for the series of CeM_2Al_{10} compounds. The main peak in these spectra originates mainly from the M-element d states hybridized with other valence band electrons. The results shown in figure 1 indicate the different electronic structure of $CeRu_2Al_{10}$ and $CeOs_2Al_{10}$ in respect to $CeFe_2Al_{10}$. The Fe 3d states of $CeFe_2Al_{10}$ are located near the Fermi level, whereas the Ru 4d states of $CeRu_2Al_{10}$ and Os 5d states of $CeOs_2Al_{10}$ are widely distributed in the valence bands. Our results well agree with very recent local-density approximation (LDA) band structure calculations [13], and suggest that hybridization between the Fe 3d and Ce 4f states is stronger than that in the case of Ru 4d and Os 5d.

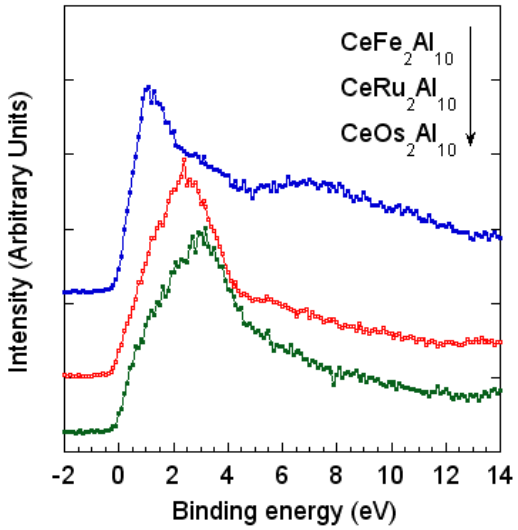

Figure 1. Valence band XPS spectra for CeM_2Al_{10}, M = Fe, Ru, and Os.

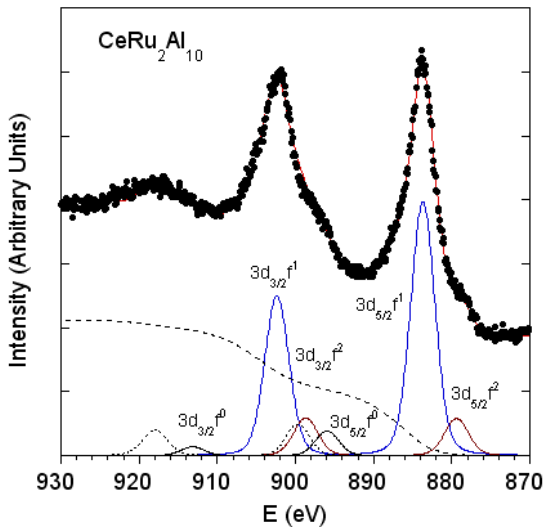

Figure 2. The Ce 3d XPS spectra for $CeRu_2Al_{10}$. The f^n (n = 0, 1, 2) components are separated on the basis of the Doniach-Šunjićtheory [16]. The dotted lines indicate the plasmon excitations, the second dotted line shows the background. Similar spectra were measured for CeM_2Al_{10}, M = Os, Fe.

The XPS spectra of the 3d core levels provide detailed information about the 4f shell configuration and the f-conduction-electron hybridization. Due to many-body interactions, the Ce 3d XPS spectra show different final states depending on the occupation of the f shell; f^0, f^1 and f^2 (detailes in [14]). Figure 2 displays the Ce 3d XPS spectra for the series of CeM_2Al_{10} compounds. All the final state-

contributions f^n are observed in the spectra. The quantitative analysis of the Ce 3d XPS spectra was performed on the basis of the Gunnarsson-Schönhammer [14] model. The hybridization width $\Delta_{cf} = \pi V^2 N(E_F)$, where $N(E_F)$ is the density of states (DOS) at the Fermi level E_F, was estimated from the ratio of the proper intensities $I(f^2)/[I(f^1) + I(f^2)]$. The analysis suggests that the hybridization Δ_{cf} is ~56 meV for $CeRu_2Al_{10}$ and ~58 meV for $CeOs_2Al_{10}$, while for $CeFe_2Al_{10}$ $\Delta_{cf} \approx 76$ meV is distinctly increased. Although the deconvolution of the XPS spectra as well as the model are subject to error (less than 20%, [15]) the trend in increasing of the hybridization effect in the order of Ru ≈ Os → Fe is clear. The f^0 components in the 3d XPS spectra of CeM_2Al_{10} also shown in the figure 2, marks the fractional valence character of Ce atoms. From the GS method the fractional valence of Ce is roughly equal to the intensity ratio $\nu = I(f^0)/[I(f^0) + I(f^1) + I(f^2)]$, which is ~0.04 for $CeRu_2Al_{10}$ and $CeOs_2Al_{10}$ and $\nu \approx 0.03$ for $CeFe_2Al_{10}$. Such a small value of ν is characteristic of the correlated and almost localized f-electron systems.

The stability of paramagnetic vs. magnetic ground state in the Kondo-lattice limit is strongly dependent on the site hybridization magnitude V and the number n_e of electrons per site. The Doradziński-Spałek (DS) phase diagram [2] on the V-n_e can be used for qualitative interpretation of the ground state of the CeM_2Al_{10} series on the base of the XPS experimental data. Considering, that the number of the conduction electrons $n_e = n_f + n_c \approx 2$, the large hybridization energy $V \sim [\Delta_{cf}/N(E_F)]^{1/2}$ decides about the KI state formation. For the series CeM_2Al_{10}, energy Δ_{sf} is about 20 meV larger for $CeFe_2Al_{10}$ in respect to Δ_{cf} of $CeRu_2Al_{10}$ and $CeOs_2Al_{10}$. One expects the small DOS at E_F for the Kondo-gap state in $CeFe_2Al_{10}$ and large value of hybridization energy V. Therefore, in DS diagram $CeFe_2Al_{10}$ would be located in the Kondo-insulator region. The transition from KI region to a metallic region can be possible vs. the change of hybridization energy V, this would be a case in the series of CeM_2Al_{10} compounds. The most probable state for $CeRu_2Al_{10}$ and $CeOs_2Al_{10}$, predicted from the DS phase diagram is the antiferromagnetic Kondo insulator, or semimetallic antiferromagnet with a pseudogap at the Fermi energy.

3. $CeFe_2Al_{10}$, universal scaling $\chi\rho = const$

Recently, it was reported [17,18] that the formation of the Kondo-insulator gap is due to the presence of collective spin-singlet Kondo state, which is singled out by magnetic susceptibility $\chi(T) \to 0$ with decreasing temperature, and activated behaviour of the resistivity $\rho(T)$. In consequence, the universal scaling law $\chi(T)\rho(T) = const$ completes the definition of a Kondo semiconductor. Figure 3 shows that the $\chi(T)\rho(T) = const$ behaviour is also observed for $CeFe_2Al_{10}$, which is a typical paramagnetic Kondo insulator.

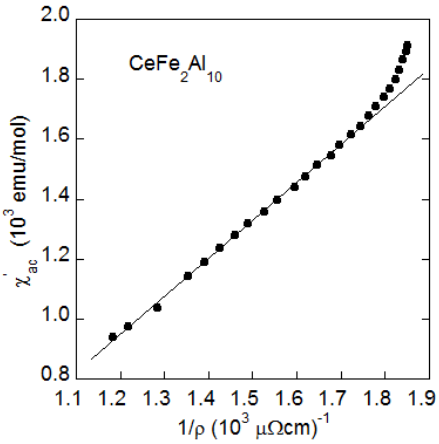

Figure 3. The ac susceptibility χ'_{ac} as a function of the inverse resistivity ρ^{-1} for $CeFe_2Al_{10}$. The $\chi(T)\rho(T) = const$ behaviour is observed between ~ 6 K and 20 K. χ'_{ac} is subtracted by impurity effect (yC/T; $y = 0.008$ and C is Curie constant for paramagnetic Ce).

The main conclusions from our magnetic and XPS data are the following: $CeFe_2Al_{10}$ obeys the features characteristic of the known paramagnetic Kondo insulators (see Ref. [19]). The analysis of the Ce 3d XPS spectra suggests that the hybridization energy between the f and conduction electron states

is the largest for $CeFe_2Al_{10}$ inside the series of CeM_2Al_{10} compounds, where M = Ru, Os, and Fe. The magnetic/paramagnetic ground state properties of CeM_2Al_{10} can be grasped by the periodic Anderson model. This model suggests the paramagnetic KI state of $CeFe_2Al_{10}$, whereas for the remaining compounds (Ru, Os) the most probable seems to be an antiferromagnetic KI state. The model is, however, too simple to explain the nature of the phase transition below T^*.

Acknowledgments
The work was supported by the Ministry of Science and Higher Education within the research project No. N N202 032137.

References
[1] For review, see Aeppli G and Fisk Z 1992 *Comments Condens. Matter. Phys.* **16**, 155
[2] Doradziński R and Spałek J 1998 *Phys. Rev.* B **58** 3293
[3] Ekino T, Takabatake T, Tanaka H, and Fujii H 1995 *Phys. Rev. Lett.* **75** 4262
[4] Sanchez-Castro C, Bedell K S, and Cooper B R 1993 *Phys. Rev.* B **47** 6879
[5] Malik S K and Adroja D T 1991 *Phys. Rev.* B **43** 6277
[6] Hundley M F, Canfield P C, Thompson J D, and Fisk Z 1990 *Phys. Rev.* B **42** 6842
[7] Strydom A M 2009 *Physica* B **404** 2981
[8] Nishioka T, Kawamura Y, Takesaka T, Kobayashi R, Kato H, Matsumura M, Kodama K, Matsubayashi K, and Uwatoko Y 2009 *J. Phys. Soc. Jpn.* **78** 123705
[9] Muro Y, Motoya K, Saiga Y, and Takabatake T 2010 *J. Phys.: Conf. Ser.* **200** 12136
[10] Khalyavin D D, Hillier A D, Adroja D T, Strydom A M, Manuel P, Chapon L C, Peratheepan P, Knight K, Deen P, Ritter C, Muro Y, and Takabatake T 2010 *Phys. Rev.* B **82** 100405
[11] Matsumura M, Kawamura Y, Edamoto S, Takesaka T, Kato H, Nishioka T, Tokunaga V, Kambe S, and Yasuoka H 2009, *J. Phys. Soc. Jpn.* **78** 123713
[12] Kimura S, Iizuka T, Miyazaki H, Irizawa A, Muro Y, and Takabatake T 2011 *Phys. Rev. Lett.* **106** 56404
[13] Kimura S, Iizuka T, Miyazaki H, Hajri T, Matsunami M, Mori T, Irizawa A, Muro Y, Kajino J, and Takabatake T 2011 *Phys. Rev*. B **84** 165125
[14] Gunnarsson O, Schönhammer K 1983 *Phys. Rev.* B **28** 4315; Fuggle J C, Hillebrecht F U, Zolnierek Z, Lässer R, Freiburg Ch, Gunnarsson O, and Schönhammer K 1983 *Phys. Rev.* B **27** 7330
[15] Ślebarski A, Zawada T, Spałek J, and Jezierski A 2004 *Phys. Rev.* B **70** 235112
[16] Doniach S and Šunjić M 1970 *J. Phys.* C **3** 286
[17] Ślebarski A and Spałek J 2005 *Phys. Rev. Lett.* **95** 46402
[18] Spałek J, Ślebarski A, Goraus J, Spałek L, Tomala K, Zarzycki A, and Hackerem A 2005 *Phys. Rev.* B **72** 155112
[19] Spałek J and Ślebarski A 2011 *J. Phys.:Conf. Ser.* **273** 012055